# Effects of α-Tubulin K40 Acetylation and Detyrosination on Kinesin-1 Motility in a Purified System

Neha Kaul,[†*] Virupakshi Soppina,[‡] and Kristen J. Verhey[‡]
[†]Department of Mechanical Engineering and [‡]Department of Cell and Developmental Biology, University of Michigan, Ann Arbor, Michigan

ABSTRACT Long-range transport in cells is achieved primarily through motor-based transport along a network of microtubule tracks. Targeted transport by kinesin motors can be correlated with posttranslational modifications (PTMs) of the tubulin subunits in specific microtubules. To directly examine the influence of specific PTMs on kinesin-1 motility, we generated tubulin subunits that were either enriched in or lacking acetylation of α-tubulin lysine 40 (K40) or detyrosination of the α-tubulin C-terminal tail. We show that K40 acetylation does not result in significant changes in kinesin-1's landing rate or motility parameters (velocity and run length) across experimental conditions. In contrast, detyrosination causes a moderate increase in kinesin-1's landing rate. The fact that the effects of detyrosination are dampened by prior K40 acetylation indicates that the combination of PTMs may be an important aspect of the functional output of microtubule heterogeneity. Importantly, our results indicate that the moderate influences that single PTMs have on kinesin-1 in vitro do not explain the strong correlation between specific PTMs and kinesin-1 transport in cells. Thus, additional mechanisms for regulating kinesin-1 transport in cells must be explored in future work.

## INTRODUCTION

Intracellular transport is essential for fundamental cellular processes, including cell migration, compartmentalization, polarization, and division. Targeted transport requires the delivery of cellular components to specific locales by motor proteins that move along microtubule tracks. Although the force-generating and cargo-binding aspects of kinesin motors have been characterized (1,2), less is known about how motors deliver cargoes such as vesicles, RNA particles, and organelles with spatial precision to specific locales (3–5). The pathological outcome of misregulated transport manifests as early signs of neurodegenerative disease (6,7).

Although all microtubules are composed of αβ-tubulin heterodimers, there are several different mechanisms for generating microtubule heterogeneity in cells, including the incorporation of different tubulin isoforms, binding of microtubule-associated proteins (MAPs), and posttranslational modifications (PTMs) of tubulin subunits (8,9). Recent work has suggested that tubulin PTMs could provide a dynamic microtubule labeling system. Most tubulin PTMs, including detyrosination and polyglutamylation, occur on the tubulin C-terminal tails (CTTs) which are exposed on the surface of the microtubule. These PTMs are thus positioned to influence a variety of microtubule-based functions in cells, including targeted transport of cellular components by kinesin motors (10,11). In contrast, acetylation of α-tubulin at lysine-40 (K40) occurs on a loop that is located in the microtubule lumen (12). PTMs of tubulin and their enzymes have been implicated in the pathology of a variety of neurodegenerative diseases (11,13,14).

Much of the work on kinesins and tubulin PTMs has focused on kinesin-1 because this motor associates preferentially with PTM-marked microtubules in cells, whereas kinesin-2 and kinesin-3 motors show no selectivity for PTM-marked tracks (15). Specifically, kinesin-1 shows preferential binding to microtubules in cells containing α-tubulin subunits marked by K40 acetylation and/or CTT detyrosination (15–17). Hyperacetylation of cellular microtubules can cause misregulation of kinesin-1 transport and rescue the transport deficit in Huntington's disease (18–20). However, K40 acetylation is not sufficient to direct kinesin-1 transport to the axonal compartment in neuronal cells (21). Rather, detyrosination provides an axonal cue for selective kinesin-1 transport (17).

To directly study the effects of α-tubulin K40 acetylation and CTT detyrosination on kinesin-1 motility, we generated tubulin subunits that were enriched for or depleted in these modifications. We used microtubules polymerized from these tubulins in single-molecule motility experiments with a constitutively active version of kinesin-1. Our results indicate that although PTMs can directly influence the interaction between the motor and microtubules, the modest effects are not sufficient to account for the correlations between microtubule PTMs and kinesin-1 transport in cells.

## MATERIALS AND METHODS

### Cloning, expression, and purification of *Rn*KHC(1-560)

We used a constitutively active version of the kinesin heavy chain (KHC) subunit of kinesin-1 containing amino acids 1–560 of rat KIF5C for our experiments. For expression in mammalian cells, *Rn*KHC(1-560) was tagged with three tandem monomeric Citrine (mCit) fluorescent proteins (FPs) as described previously (22). KHC(1-560)-3xmCit was expressed in COS-7 cells and cell lysates were prepared as described previously (22). COS-7

*Submitted December 17, 2013, and accepted for publication May 8, 2014.*

*Correspondence: nehakaul@email.unc.edu

Neha Kaul's present address is Department of Pharmacology, UNC School of Medicine, Chapel Hill, North Carolina

Editor: Ram Dixit.



0006-3495/14/06/2636/8 $2.00

http://dx.doi.org/10.1016/j.bpj.2014.05.008

(monkey kidney fibroblast; ATCC) cells were grown in Dulbecco's modified Eagle's medium (DMEM) + 10% fetal bovine serum (FBS) and 2 mM L-glutamine at 37°C with 5% $CO_2$, and transfected using Expressfect (Denville Scientific, South Plainfield, NJ). Kinesin-1 expressed in *E. coli*, KHC(1-560)-EGFP, was tagged with an EGFP for visualization and a 6x-His tag for affinity purification as described previously (23,24). Following Ni-NTA column purification, the KHC(1-560)-EGFP motor was further purified by microtubule affinity purification (23). The purified motors were aliquoted and flash-frozen for storage at −80°C. No differences in motility parameters were observed between KHC(1-560) motors from mammalian cells lysates and those purified from bacterial cells.

## Tubulin purification and enzymatic treatment

Tubulin was purified from bovine brains or from HeLa S3 cells (ATCC, Manassas, VA) according to published protocols (25,26). HeLa S3 cells were grown by sequential dilution of cells in minimum essential medium-Joklik modification (Sigma-Aldrich, St. Louis, MO) + 10% FBS at 37°C with 5% $CO_2$. All cells were grown in the presence of 50 U/mL penicillin/streptomycin, and 10 L of suspension culture yielded 2.5 mg of soluble HeLa tubulin. The tubulin was resuspended in BRB80 (80 mM PIPES, pH 6.8, 1 mM $MgCl_2$, 1 mM EGTA) before it was aliquoted and flash-frozen for storage at −80°C. A 7.5% SDS-PAGE gel was run with samples from the purification procedure to verify the purity of the tubulin (Fig. S1 in the Supporting Material).

For acetylation and deacetylation of tubulin, plasmids for expression of recombinant GST-MEC-17 (pGEX-MEC-17 (27) (a gift from Jacek Gaertig, University of Georgia)) and His_SIRT2 (pHEX-His-SIRT2 (28), a gift from Eric Verdin, UCSF)) were expressed in *E. coli* and the proteins were purified as described previously (12). For detyrosination, HeLa tubulin was incubated with 10 $\mu$g/mL carboxypeptidase A (CPA; Sigma-Aldrich) on ice for 20 min. Enzyme-treated tubulins were processed through two temperature-dependent cycles of polymerization and depolymerization to remove any polymerization-incompetent tubulin generated during enzyme treatment (Fig. S2). Tubulin modification was confirmed by immunoblotting with the monoclonal antibody 6-11B-1, which recognizes K40-acetylated $\alpha$-tubulin (T6793; Sigma-Aldrich) or a polyclonal antibody that recognizes detyrosinated $\alpha$-tubulin (AB3201; Millipore, Billerica, MA).

## Single-molecule motility assays using total internal reflection fluorescence microscopy

Motility assays were performed on a Zeiss Axiovert 135 microscope modified to allow total internal reflection fluorescence (TIRF) microscopy using a 100×/1.45 N.A. $\alpha$-Plan-Fluar objective. A 488 nm Ar-ion laser was used for excitation. The emission was chromatically separated using a dual-view imaging device (DV2; Photometrics, Tucson, AZ) with T585lpxr dichroic and HQ510, ET525/50m filters (Chroma Technology, Bellows Falls, VT), and images were collected on an EMCCD camera (Cascade 512B; Photometrics, Tucson, AZ).

Microtubules polymerized in the presence of 1 mM GTP using 4 mg/mL of untreated or treated tubulins and stabilized with 10 $\mu$M taxol in BRB80 were flowed into the chamber and allowed 5 min to adhere before the chamber was blocked with 1 mg/mL bovine serum albumin (BSA). Recombinant kinesin motors (~10 nM) or cell lysates containing expressed motors were then added to the chamber in P12 buffer (12 mM PIPES, pH 6.8, 2 mM $MgCl_2$, 1 mM EGTA) supplemented with 1 mM $MgCl_2$, 2 mM ATP, 1 mg/mL BSA, 10 mM glucose, 1.65 mg/mL glucose oxidase, 0.27 mg/mL catalase, and 143 mM $\beta$-mercaptoethanol. For motility assays in a more physiological buffer, buffer conditions were 25 mM HEPES/KOH pH 7.4, 115 mM KOAc, 5 mM NaOAc, 5 mM $MgCl_2$, 0.5 mM EGTA.

For some assays, treated tubulins were differentially labeled before they were added to the assay. Succinimidyl esters of Alexa488 (Life Technologies, Grand Island, NY) and Atto590 (ATTO-TEC, Siegen, Germany) dyes were used to label deacetylated and acetylated tubulin, respectively. The tubulin was cycled through two cycles of polymerization and depolymerization to remove incompetent tubulin from the preparation. The labeled-to-unlabeled tubulin ratios were 1:60 and 1:15 for Alexa488- and Atto590-labeled tubulin, respectively. Differentially labeled microtubules were mixed together and then introduced into the same flow chamber.

## Data collection and analysis

To simultaneously capture motility events on Atto590-labeled acetylated and Alexa488-labeled deacetylated microtubules, a still image of each microtubule population was first acquired in the red and green channels. The fluorescence from the Alexa488 dye decayed rapidly in the presence of the 488 nm excitation light, making the green channel available for recording video sequences of 3xmCit- or EGFP-labeled KHC(1-560) motility events. The captured still images were then used to identify the acetylated versus deacetylated microtubule tracks for each kinesin event traced during data analysis. In assays using unlabeled tubulins, the microtubules were identified after imaging by generating standard deviation (SD) maps of fluorescent KHC(1-560) motility from the movie recording as described previously (22). Data were collected from several locations per flow chamber, each of which contained three to four microtubules in the field of view.

The single-molecule motility data were analyzed using a custom-written MATLAB routine (The MathWorks, Natick, MA). The program identifies diffraction-limited fluorescent spots within a selected region of interest and determines the exact location of the centroid of each spot based on its fit to a Gaussian intensity profile. Individual fluorescent spots are recognized as spots of interest if they appear and track in subsequent frames in a manner consistent with a motility event. The velocities and run lengths of individual spots are computed from frame-by-frame coordinates. All runs above 0.15 $\mu$m were included in the MATLAB analysis. Histograms of the population data were generated by plotting the number of events observed against binned values of the data. The profile of the velocity histogram was fit to a Gaussian distribution using the function F = A × exp(−0.5 × ((centers − $\mu$)./s) .^2) ./ (s × sqrt(2 × $\pi$)), where A is the amplitude, $\mu$ is the mean, and s is the SD. The mean value of the distribution represents the average speed of the observed single motor events. The cumulative distribution function (CDF) of the run lengths (ecdf function in MATLAB) was fit to an exponential curve defined by the function F = 1 − exp((minRL − RLx)./t), where minRL = 0.15 $\mu$m and RLx is the output of the ecdf function. The decay constant from the fit, t, yields the mean run length. All histograms for the velocity and run length data were characterized by excellent fits ($R^2 > 0.93$). The landing rate of kinesin motors on microtubules was computed by quantifying the number of motile events on a selected microtubule in a recorded movie divided by the length of the microtubule and the length of the movie to obtain a landing rate with the units events/$\mu$m/min. From this, a relative Kd was calculated as the $k_{off}/k_{on}$, where $k_{off}$ = the average velocity/average run length and the relative $k_{on}$ = the landing rate. To determine statistical significance between data sets, a two-sample *t*-test statistic was calculated in MATLAB. Data were randomly resampled by bootstrapping to arrive at a *p*-value for comparing the means. A *p*-value < 0.01 was used to reject the null hypothesis.

# RESULTS

## Acetylation of $\alpha$-tubulin K40 and its effect on kinesin-1 motility

We first set out to test whether acetylation of K40 in $\alpha$-tubulin directly affects kinesin-1 motility. To do this, we polymerized microtubules from purified bovine brain tubulin treated with either recombinant deacetylase SIRT2

(28) or acetyltransferase MEC-17 (27) enzymes. To verify the effects of enzymatic treatment, immunoblotting was carried out with a monoclonal antibody (6-11B-1) that specifically recognizes the acetylated K40 residue. Consistent with previous reports (27–29), SIRT2 treatment resulted in a complete loss of K40 acetylation, whereas MEC-17 treatment resulted in a 1.3-fold increase in the total levels of K40 acetylation (Fig. 1 *A*).

The motility of kinesin-1 motors along microtubules polymerized from either deacetylated or acetylated tubulins was determined in single-molecule motility assays. To directly compare the motility of KHC(1-560)-3xmCit on deacetylated and acetylated microtubules, the treated tubulins were first differentially labeled with fluorescent dyes to distinguish them in the motility assay. The motors were thus introduced into a flow chamber containing Alexa488-labeled deacetylated and Atto590-labeled acetylated microtubules. Kinesin-1 motors were observed to move along both deacetylated and acetylated microtubules (Fig. 1 *B*; Movies S1 and S2). Quantification of the motility events showed that the landing rate for kinesin-1, calculated as the number of binding events observed on a given length of microtubule per unit time, was 3.82 ± 1.03 events/$\mu$m/min (relative Kd = 2.94 events/$\mu$m; Table 1) on deacetylated microtubules, and 3.71 ± 1.51 events/$\mu$m/min (relative Kd = 2.81 events/$\mu$m; Table 1) on acetylated microtubules (Fig. 1 *C*; Table 1, $p = 0.72$). Upon landing, the motor moved with a mean velocity of 0.65 ± 0.17 $\mu$m/s on deacetylated microtubules and 0.64 ± 0.13 $\mu$m/s on acetylated microtubules (Fig. 1 *D*; Table 1; $p < 0.01$). Kinesin-1 exhibited a mean run length of 0.532 ± 0.001 $\mu$m (mean + SE) on deacetylated microtubules and 0.507 ± 0.001 $\mu$m on acetylated microtubules (Fig. 1 *E*; Table 1; $p < 0.01$). The changes in kinesin-1 motility observed in this purified system (a 1.5% decrease in velocity and 4% decrease in run length) do not account for changes in kinesin-1 motility that are observed in vivo.

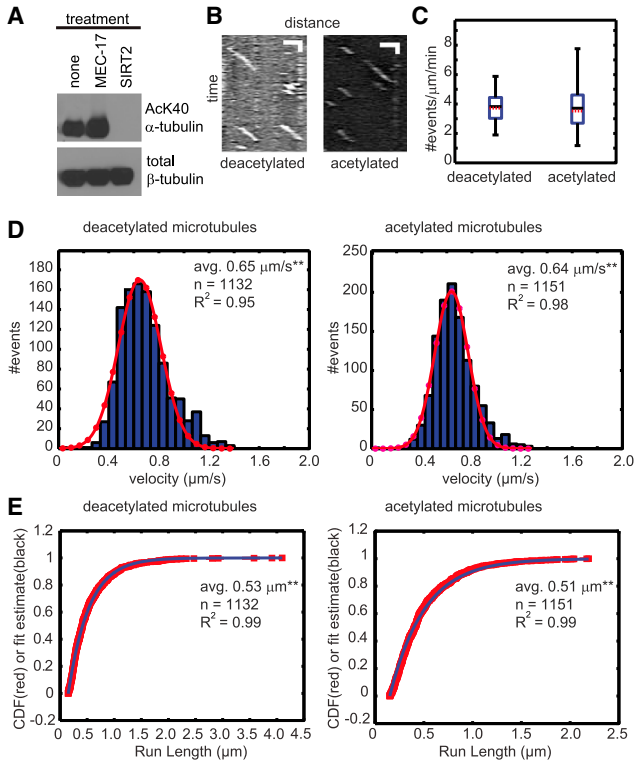


FIGURE 1 Effects of $\alpha$-tubulin K40 acetylation on kinesin-1. (*A*) Bovine brain tubulin was treated with either MEC-17 acetyltransferase or SIRT2 deacetylase enzymes and the resulting K40 acetylation levels were analyzed by western blot using antibodies that specifically recognize $\alpha$-tubulin acetylated at K-40 (6-11B-1) or total $\beta$-tubulin. (*B–E*) Microtubules polymerized from acetylated or deacetylated tubulins were differentially dye labeled and introduced into the same flow chamber for single-molecule motility assays, and the (*C*) landing rate, (*D*) velocity, and (*E*) run length of individual KHC(1-560)-3xmCit motors were measured. (*B*) Representative kymographs of kinesin-1 motility along deacetylated (*left*) and acetylated (*right*) microtubules. Vertical scale bar: 1 s; horizontal scale bar: 1 $\mu$m. (*C*) For the landing rate, the data are presented as box-whisker plots of the number of motility events per unit length of microtubule per unit time. The black line indicates the mean, the dashed red line indicates the median, the rectangle indicates the 25th-75th percentile, and the red spots indicate outlying data points. (*D*) For velocity, the data are presented as a histogram of the population and the average velocity was computed from Gaussian fits of the data (*red lines*). (*E*) For run length, the population data (*red boxes*) were plotted as CDFs and the averages were computed from exponential fits (*blue lines*). **p $\leq$ 0.01. To see this figure in color, go online.

One possible explanation for the fact that the effect of K40 acetylation in our experimental setup does not mirror in vivo changes for kinesin-1 motility is that the differential dye labeling of deacetylated and acetylated tubulins abolished any influence of acetylation on the motility properties of kinesin-1. To test this possibility, we performed control assays using unlabeled deacetylated or acetylated microtubules in separate flow cells. In this case, K40 acetylation caused a decrease in the landing rate, an increase in the mean velocity, and no significant change in the mean run length of kinesin-1 (Fig. 2 *A*; Table 1). A second possibility is that the ionic strength of the motility buffer could account for the differences between our in vitro results and previous in vivo work, because the kinesin-microtubule interaction has been shown to be dependent on the ionic strength of the motility buffer (30). Under physiological ionic strength conditions, K40 acetylation caused no significant changes in kinesin-1's landing rate, mean velocity, or mean run length (Fig. 2 *B*; Table 1). A third possibility is that the use of taxol to stabilize microtubules in our assays could alter kinesin-1 motility compared with the situation in cells. KHC(1-560)-3xmCit showed a similar landing rate and mean velocity on deacetylated and acetylated microtubules in the presence of GMPCPP to stabilize microtubules, but a decrease in the run length (Fig. 2 *C*; Table 1). These control assays demonstrate that alteration of the K40 acetylation state of $\alpha$-tubulin did not cause consistent changes in kinesin-1 motility across the experimental conditions used (Table 1). Overall, the magnitude of the changes in these experiments is small

**TABLE 1 Motility parameters for kinesin-1 on acetylated and deacetylated bovine brain microtubules under different conditions**

| | Combined Assay | | Unlabeled Tubulin | | Physiological Buffer | | GMPCPP Stabilized | |
|---|---|---|---|---|---|---|---|---|
| $\alpha$-Tubulin state | Deacetylated | Acetylated | Deacetylated | Acetylated | Deacetylated | Acetylated | Deacetylated | Acetylated |
| *n* | 1132 | 1151 | 678 | 369 | 87 | 71 | 208 | 141 |
| Landing rate (events/$\mu$m/min) | 3.82 ± 1.03 | 3.71 ± 1.51 | 7.02 ± 1.38** | 5.76 ± 0.82** | 1.32 ± 1.02 | 1.35 ± 0.75 | 5.10 ± 0.92 | 4.76 ± 0.75 |
| $K_{off}$ = Vel/RL | 1.30 | 1.32 | 1.33 | 1.40 | 1.75 | 1.75 | 1.11 | 1.27 |
| Kd (relative) | 2.94 | 2.81 | 5.29 | 4.13 | 0.69 | 0.55 | 4.61 | 3.74 |
| Change in Kd | −5% | | −22% | | −21% | | −19% | |
| Velocity ($\mu$m/s) | 0.65 ± 0.17** | 0.64 ± 0.13** | 0.61 ± 0.14** | 0.67 ± 0.14** | 0.82 ± 0.28 | 0.77 ± 0.05 | 0.73 ± 0.15 | 0.75 ± 0.14 |
| Upper 95% CI | 0.67 | 0.65 | 0.62 | 0.68 | 0.89 | 0.90 | 0.77 | 0.77 |
| Lower 95% CI | 0.63 | 0.63 | 0.60 | 0.66 | 0.74 | 0.65 | 0.69 | 0.73 |
| Run length ($\mu$m) | 0.532 ± 0.001** | 0.507 ± 0.001** | 0.457 ± 0.001 | 0.481 ± 0.002 | 0.470 ± 0.004 | 0.436 ± 0.003 | 0.663 ± 0.002* | 0.588 ± 0.004* |
| Upper 95% CI | 0.533 | 0.510 | 0.460 | 0.485 | 0.478 | 0.443 | 0.668 | 0.596 |
| Lower 95% CI | 0.530 | 0.505 | 0.455 | 0.478 | 0.464 | 0.431 | 0.661 | 0.582 |

Data are presented as mean ± SD for velocity and landing rate, and mean ± SE for run length. *n*, number of events observed; CI, confidence interval of mean. *p ≤ 0.05, **p ≤ 0.01.

and not sufficient to explain the in vivo correlation of K40 acetylation and kinesin-1 motility.

## Detyrosination of $\alpha$-tubulin CTTs and its effect on kinesin-1 motility

We next set out to directly test the effects of detyrosination on kinesin-1 motility. To obtain a population of microtubules enriched in tyrosinated $\alpha$-tubulin, we purified tubulin from HeLa cells, which contain 99.5% tyrosinated $\alpha$-tubulin (31). The tyrosinated HeLa tubulin was treated with CPA to remove the C-terminal tyrosine residue as described previously (32), thus generating detyrosinated tubulin. As shown in Fig. 3 *A*, untreated HeLa tubulin contains undetectable levels of detyrosination, whereas CPA-treated HeLa tubulin is enriched in detyrosination. Tyrosinated or detyrosinated microtubules were polymerized from these tubulins and used in motility assays with recombinant KHC(1-560)-EGFP.

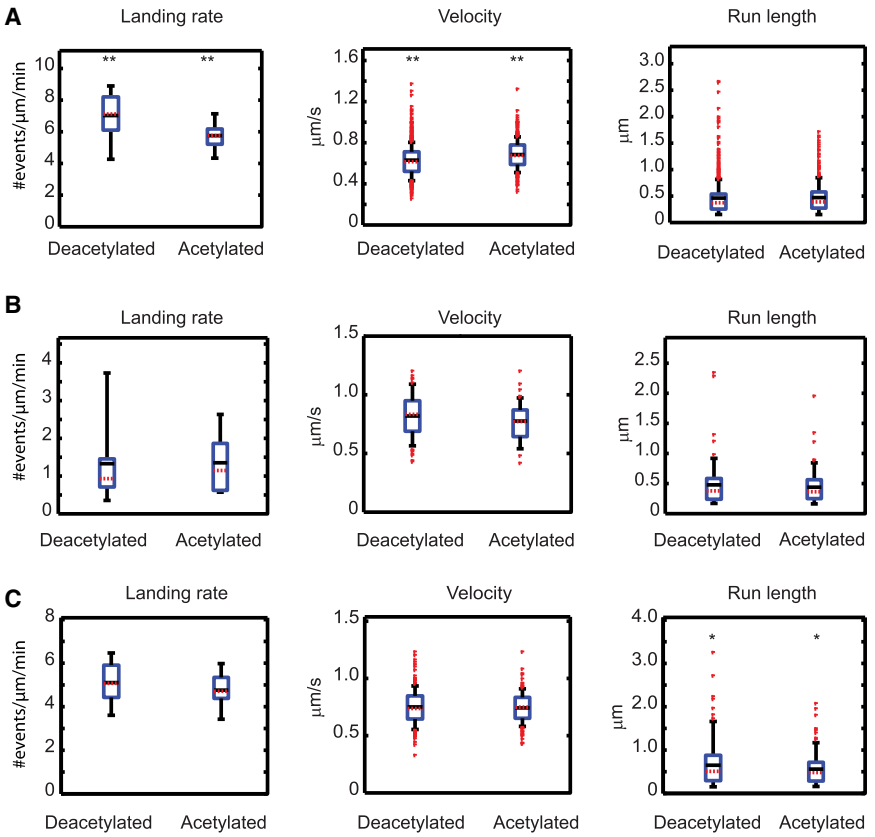


FIGURE 2 Effects of K40 acetylation on kinesin-1 under different experimental conditions. Microtubules polymerized from deacetylated or acetylated tubulins were used for single-molecule motility assays. (*A–C*) The motility of KHC(1-560)-3xmCit motors was observed on (*A*) unlabeled deacetylated or acetylated microtubules in separate flow chambers, (*B*) deacetylated or acetylated microtubules under physiological ionic strength conditions, or (*C*) taxol-free GMPCPP-stabilized deacetylated or acetylated microtubules. The data are presented as box-whisker plots. The black line indicates the mean, the dashed red line indicates the median, the rectangle indicates the 25th–75th percentile, and the red spots indicate outlying data points. *p ≤ 0.05, **p ≤ 0.01. To see this figure in color, go online.

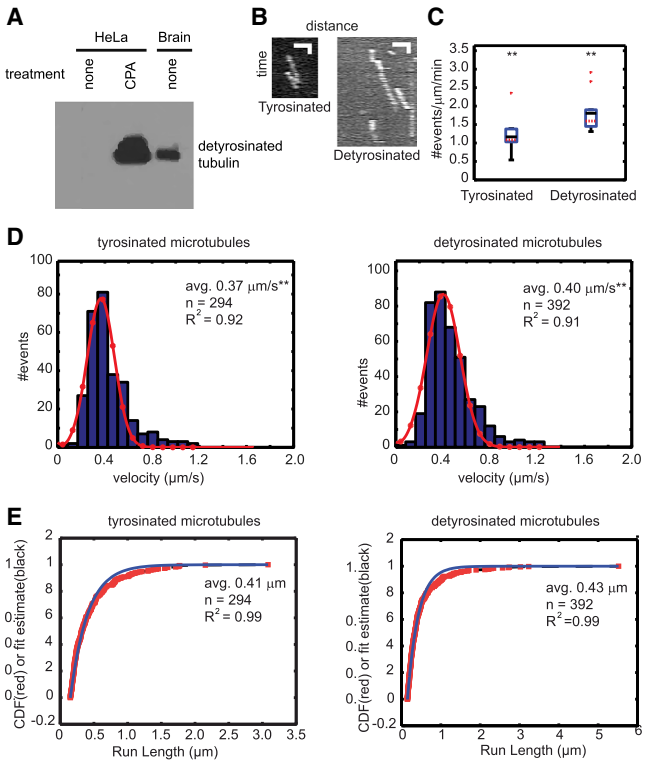


FIGURE 3 Effects of microtubule detyrosination on kinesin-1 motors. (*A*) Purified HeLa tubulin (500 ng) that was untreated or treated with CPA to detyrosinate α-tubulin (Fig. S1, lane 6, and Fig. S2, lane 7, respectively) or bovine tubulin (500 ng) was analyzed by western blotting with an antibody to detyrosinated α-tubulin. (*B–E*) Microtubules polymerized from tyrosinated or detyrosinated tubulins were used in single-molecule motility assays. (*B*) Representative kymographs of KHC(1-560)-EGFP motility along tyrosinated (*left*) and detyrosinated (*right*) microtubules. Vertical scale bar: 1 s; horizontal scale bar: 1 μm. (*C–E*) The (*C*) landing rate, (*D*) velocity, and (*E*) run length of KHC(1-560)-EGFP motors were measured on tyrosinated and detyrosinated microtubules in separate flow chambers. The data are presented as described in Fig. 1. **p ≤ 0.01. To see this figure in color, go online.

KHC(1-560)-EGFP motors were observed to move on both tyrosinated and detyrosinated microtubules (Fig. 3 *B*). Quantification of the motility data showed a statistically significant increase in the landing rate from 1.17 ± 0.50 events/μm/min on tyrosinated microtubules to 1.80 ± 0.56 events/μm/min on detyrosinated microtubules ($p \leq 0.01$; Fig. 3 *C*; Table 2). This represents a 49% increase in the relative Kd of the motor for the microtubule (from 1.30 events/μm to 1.94 events/μm upon detyrosination; Table 2). Detyrosination also caused a slight but statistically significant increase in KHC(1-560)-EGFP velocity (0.37 ± 0.11 μm/s on tyrosinated microtubules versus 0.40 ± 0.14 μm/s on detyrosinated microtubules; $p < 0.01$; Fig. 3 *D*; Table 2), but no significant change in run length (0.409 ± 0.002 μm on tyrosinated microtubules versus 0.428 ± 0.001 μm on detyrosinated microtubules; $p = 0.14$; Fig. 3 *E*; Table 2). Based on these results, we conclude that detyrosination of the α-tubulin CTT primarily affects the initial interaction of kinesin-1 motors with the microtubule track by increasing their landing rate.

## Effects of combined α-tubulin acetylation and detyrosination on kinesin-1 motility

We next considered the possibility that the two α-tubulin modifications, K40 acetylation and CTT detyrosination, may work in conjunction with each other. This is supported by the fact that in multiple cell types, microtubules are often colabeled with antibodies to α-tubulin K40 acetylation and detyrosination (31,33–35).

Tyrosinated tubulin purified from HeLa cells was treated with recombinant MEC-17 to generate tyrosinated+acetylated tubulin. A fraction of this tubulin was then treated with CPA to generate detyrosinated+acetylated tubulin. Single-molecule motility assays were performed to measure the motility parameters of kinesin-1 on both types of microtubules. Detyrosination of previously acetylated α-tubulin caused an increase in the landing rate of KHC(1-560)-EGFP from 1.48 ± 0.40 events/μm/min on tyrosinated+acetylated microtubules to 1.75 ± 0.52 event/μm/min on detyrosinated+acetylated microtubules (Fig. 4 *A*; Table 2); however, this increase was not statistically significant ($p = 0.30$). This represents a 28% increase in the relative Kd of the motor for the microtubule (from 1.67 event/μm on tyrosinated+acetylated microtubules to 2.13 event/μm on acetylated + detyrosinated microtubules; Table 2). Whereas detyrosination caused an increase in motor velocity, detyrosination+acetylation resulted in a decreased velocity (0.47 ± 0.13 μm/s on tyrosinated+acetylated microtubules and 0.40 ± 0.12 μm/s on detyrosinated+acetylated microtubules; $p < 0.01$; Fig. 4 *B*; Table 2), whereas the mean run length was unchanged (0.520 ± 0.000 μm on tyrosinated+acetylated microtubules and 0.502 ± 0.001 μm on detyrosinated+acetylated microtubules; $p = 0.43$; Fig. 4 *C*; Table 2). These results indicate that K40 acetylation dampens the effects of detyrosination on the kinesin-1 landing rate. Therefore, PTMs may act in conjunction with each other to affect the overall landing rate of kinesin-1.

## DISCUSSION

Previous studies in cells have demonstrated a strong correlation between the direction of kinesin-1 transport and the presence of specific PTMs on subsets of microtubule tracks (15–21). Findings from these studies predicted that individual PTMs would directly impact the motor. Using a purified system to examine the effects of specific tubulin PTMs on the motility of a kinesin motor, we found that neither acetylation nor detyrosination greatly affected kinesin-1 velocity or run length; however, detyrosination did increase the landing rate of kinesin-1. Yet, these in vitro results using a purified system do not recapitulate the track selectivity of kinesin-1 that is observed in cells. The most likely scenario

**TABLE 2 Motility parameters for kinesin-1 on tyrosinated and detyrosinated tubulins from HeLa cells**

| Treatment | None | CPA | MEC-17 | MEC-17 + CPA |
|---|---|---|---|---|
| $\alpha$-Tubulin state | Tyrosinated | Detyrosinated | Tyrosinated + acetylated | Detyrosinated + acetylated |
| *n* | 294 | 392 | 1461 | 854 |
| Landing rate (events/$\mu$m/min) | 1.17 ± 0.50** | 1.80 ± 0.56** | 1.48 ± 0.40 | 1.76 ± 0.52 |
| $K_{off}$ = Vel/RL | 0.90 | 0.93 | 0.90 | 0.80 |
| Kd (relative) | 1.30 | 1.94 | 1.67 | 2.13 |
| Change in Kd | | +49% | | +28% |
| Velocity ($\mu$m/s) | 0.37 ± 0.11** | 0.40 ± 0.14** | 0.47 ± 0.13** | 0.40 ± 0.12** |
| Upper 95% CI | 0.39 | 0.43 | 0.48 | 0.42 |
| Lower 95% CI | 0.34 | 0.37 | 0.45 | 0.38 |
| Run length ($\mu$m) | 0.409 ± 0.002 | 0.428 ± 0.001 | 0.520 ± 0.000 | 0.502 ± 0.001 |
| Upper 95% CI | 0.412 | 0.431 | 0.521 | 0.503 |
| Lower 95% CI | 0.405 | 0.426 | 0.520 | 0.501 |

Data are presented as mean ± SD for velocity and landing rate, and mean ± SE for run length. *n*, number of events observed; CI, confidence interval of mean. *p ≤ 0.05, **p ≤ 0.01.

would appear to be that individual MAPs influence kinesin-1 binding and motility in cells (9), a possibility that deserves further experimental focus.

Our findings on K40 acetylation are consistent with two recent reports that found no significant differences in kinesin-1 binding to or motility along acetylated versus deacetylated microtubules (12,24). In this work, we extended the scope of those studies by measuring the landing rate on and the relative Kd for acetylated and deacetylated microtubules. Thus, there is a good consensus that K40 acetylation, which is located on the luminal side of the microtubule (12), does not directly influence motor binding or motility on the outside of the microtubule. How can this finding be reconciled with previous observations suggesting that K40 acetylation positively influences the binding of kinesin-1 motors and/or transport of kinesin-1 cargoes in cells (15,17–20)? Previous work relied on either hyperacetylation of cellular microtubules via chemical inhibition of deacetylase enzymes (17–20) or expression of mutant tubulins that could not be acetylated (19). With regard to the former, deacetylase inhibitors are likely to cause general alterations in protein acetylation, including changes in tubulin beyond K40 acetylation. Indeed, recent work has shown that $\beta$-tubulin can also be acetylated (36), although the effects of deacetylase inhibitor treatment on the site are not known. With regard to the latter, the expression of mutant tubulins could alter microtubule structure in cells and thereby influence kinesin binding and/or motility. It thus appears that the functional output of cellular microtubules recognized by the anti-acetylK40 antibody (6-11B-1) cannot be recapitulated in purified systems. In support of this, loss of the acetyltransferase MEC-17 in *C. elegans* was shown to lead to a change in protofilament number (37,38), whereas cryo-electron microscopy analysis revealed no structural differences between microtubules polymerized from acetylated and deacetylated tubulins in vitro (39). The functional output of K40 acetylation in cells may thus be due to local changes in $\alpha$-tubulin conformation and/or subunit interactions (12,37) as well as the recruitment of specific MAPs (9).

Our results provide the first analysis (to our knowledge) of kinesin-1 motility along tyrosinated and detyrosinated mammalian microtubules. We find that the major influence of $\alpha$-tubulin detyrosination is on the landing rate of kinesin-1 on microtubules (Table 2). This is consistent with previous work showing that kinesin-1 binds more tightly to CPA-treated tubulins (16,17,40), and recent work showing that kinesin-1 displays similar motility parameters (velocity and processivity) on microtubules polymerized from yeast tubulins containing tyrosinated or detyrosinated human $\alpha$-tubulin CTTs (41). Can the increased relative Kd of kinesin-1 on detyrosinated microtubules in vitro explain the selective transport of kinesin-1 along detyrosinated microtubules in cells? Knockdown of tubulin tyrosine ligase (TTLL1, the enzyme that retyrosinates $\alpha$-tubulin) results in increased levels of detyrosinated tubulin and alters the trafficking of kinesin-1 motors in polarized hippocampal neurons (17). However, it seems unlikely that detyrosination provides the only cue to kinesin-1 for selective transport, as kinesin-1 motility can be observed along tyrosinated microtubules in cells (15) and knockout of *Ttll1* in mice does not impair neuronal polarization (42). It also appears that the combination of PTMs may be important for their functional output, as the effect of detyrosination on kinesin-1's landing rate was dampened when the tubulin was previously acetylated (an increase of 49% in the relative Kd for CPA treatment alone versus an increase of 28% for previously acetylated microtubules; Table 2). Thus, the primary effect of detyrosination is to regulate the binding affinity of kinesin-1 for microtubules and not the motility properties of the motor once it is bound. Mechanistically, modulation of the landing rate offers an elegant and simple way to regulate transport because it does not require changes in the ATP hydrolysis rate of the motor, as would be required for changing the motor velocity.

Taken together, our results indicate that the view of single PTMs directly regulating kinesin-1 transport is too simplistic; rather, multiple inputs regulate the interaction of kinesin-1 with microtubules. In cells, the initial interaction

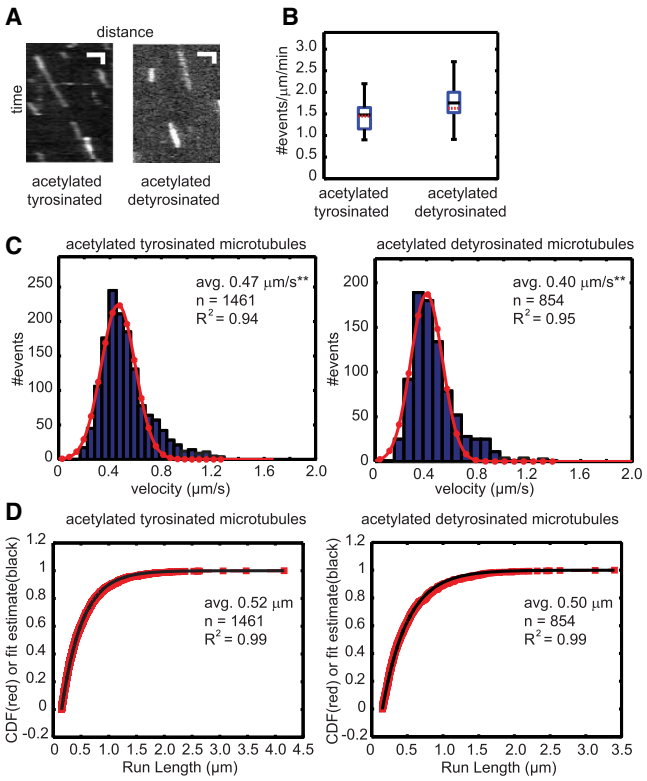


FIGURE 4 The effects of detyrosination on kinesin-1's landing rate were dampened by previous acetylation of K40. Purified HeLa tubulin was treated with MEC-17 to generate acetylated+tyrosinated microtubules and then a portion was further treated with CPA to generate acetylated+detyrosinated microtubules. (*A–D*) Microtubules polymerized from these tubulin types was used in single-molecule motility assays. (*A*) Representative kymographs of KHC(1-560)-EGFP motility along acetylated+tyrosinated (*left*) or acetylated+detyrosinated (*right*) microtubules. Vertical scale bar: 1 s; horizontal scale bar: 1 $\mu$m. (*B–D*) The motility of individual KHC(1-560)-EGFP motors was observed and used to measure the (*B*) landing rate, (*C*) velocity, and (*D*) run length of the motors. The data are presented as described in Fig. 1. **p $\leq$ 0.01. To see this figure in color, go online.

of kinesin-1 with microtubules is likely to be influenced by a combination of PTMs, particularly detyrosination, as well as MAPs and perhaps tubulin isoforms (9). Further work using the isolated assay system that we have developed will provide insight into how specific alterations of tubulin subunits can influence kinesin-1 motors in vitro, which in turn will further our understanding of how PTMs influence cellular events such as the movement of motors and their cargoes in cells.

## SUPPORTING MATERIAL

Two figures and two movies are available at http://www.biophysj.org/biophysj/supplemental/S0006-3495(14)00505-0.

We thank Chloe Bulinski (Columbia University), Edgar Meyhofer (University of Michigan), and members of the Verhey and Meyhofer labs for helpful discussions.

This work was supported by NIH grants RO1GM070862 and RO1GM083254.

## REFERENCES

1. Block, S. M. 2007. Kinesin motor mechanics: binding, stepping, tracking, gating, and limping. *Biophys. J.* 92:2986–2995.
2. Vale, R. D. 2003. The molecular motor toolbox for intracellular transport. *Cell.* 112:467–480.
3. Ross, J. L., M. Y. Ali, and D. M. Warshaw. 2008. Cargo transport: molecular motors navigate a complex cytoskeleton. *Curr. Opin. Cell Biol.* 20:41–47.
4. Kapitein, L. C., and C. C. Hoogenraad. 2011. Which way to go? Cytoskeletal organization and polarized transport in neurons. *Mol. Cell. Neurosci.* 46:9–20.
5. Verhey, K. J., N. Kaul, and V. Soppina. 2011. Kinesin assembly and movement in cells. *Annu. Rev. Biophys.* 40:267–288.
6. De Vos, K. J., A. J. Grierson, …, C. C. Miller. 2008. Role of axonal transport in neurodegenerative diseases. *Annu. Rev. Neurosci.* 31: 151–173.
7. Franker, M. A., and C. C. Hoogenraad. 2013. Microtubule-based transport—basic mechanisms, traffic rules and role in neurological pathogenesis. *J. Cell Sci.* 126:2319–2329.
8. Janke, C., and J. C. Bulinski. 2011. Post-translational regulation of the microtubule cytoskeleton: mechanisms and functions. *Nat. Rev. Mol. Cell Biol.* 12:773–786.
9. Atherton, J., A. Houdusse, and C. Moores. 2013. MAPping out distribution routes for kinesin couriers. *Biol. Cell.* 105:465–487.
10. Janke, C., and M. Kneussel. 2010. Tubulin post-translational modifications: encoding functions on the neuronal microtubule cytoskeleton. *Trends Neurosci.* 33:362–372.
11. Garnham, C. P., and A. Roll-Mecak. 2012. The chemical complexity of cellular microtubules: tubulin post-translational modification enzymes and their roles in tuning microtubule functions. *Cytoskeleton (Hoboken).* 69:442–463.
12. Soppina, V., J. F. Herbstman, …, K. J. Verhey. 2012. Luminal localization of $\alpha$-tubulin K40 acetylation by cryo-EM analysis of fab-labeled microtubules. *PLoS ONE.* 7:e48204.
13. Butler, R., and G. P. Bates. 2006. Histone deacetylase inhibitors as therapeutics for polyglutamine disorders. *Nat. Rev. Neurosci.* 7:784–796.
14. Donmez, G., and T. F. Outeiro. 2013. SIRT1 and SIRT2: emerging targets in neurodegeneration. *EMBO Mol. Med.* 5:344–352.
15. Cai, D., D. P. McEwen, …, K. J. Verhey. 2009. Single molecule imaging reveals differences in microtubule track selection between Kinesin motors. *PLoS Biol.* 7:e1000216.
16. Dunn, S., E. E. Morrison, …, M. Peckham. 2008. Differential trafficking of Kif5c on tyrosinated and detyrosinated microtubules in live cells. *J. Cell Sci.* 121:1085–1095.
17. Konishi, Y., and M. Setou. 2009. Tubulin tyrosination navigates the kinesin-1 motor domain to axons. *Nat. Neurosci.* 12:559–567.
18. Dompierre, J. P., J. D. Godin, …, F. Saudou. 2007. Histone deacetylase 6 inhibition compensates for the transport deficit in Huntington's disease by increasing tubulin acetylation. *J. Neurosci.* 27:3571–3583.
19. Reed, N. A., D. Cai, …, K. J. Verhey. 2006. Microtubule acetylation promotes kinesin-1 binding and transport. *Curr. Biol.* 16:2166–2172.
20. Tapia, M., F. Wandosell, and J. J. Garrido. 2010. Impaired function of HDAC6 slows down axonal growth and interferes with axon initial segment development. *PLoS ONE.* 5:e12908.
21. Hammond, J. W., C. F. Huang, …, K. J. Verhey. 2010. Posttranslational modifications of tubulin and the polarized transport of kinesin-1 in neurons. *Mol. Biol. Cell.* 21:572–583.
22. Cai, D., K. J. Verhey, and E. Meyhöfer. 2007. Tracking single Kinesin molecules in the cytoplasm of mammalian cells. *Biophys. J.* 92:4137–4144.

23. Case, R. B., D. W. Pierce, …, R. D. Vale. 1997. The directional preference of kinesin motors is specified by an element outside of the motor catalytic domain. *Cell.* 90:959–966.

24. Walter, W. J., V. Beránek, …, S. Diez. 2012. Tubulin acetylation alone does not affect kinesin-1 velocity and run length in vitro. *PLoS ONE.* 7:e42218.

25. Castoldi, M., and A. V. Popov. 2003. Purification of brain tubulin through two cycles of polymerization-depolymerization in a high-molarity buffer. *Protein Expr. Purif.* 32:83–88.

26. Chapin, S. J., and J. C. Bulinski. 1991. Preparation and functional assay of pure populations of tyrosinated and detyrosinated tubulin. *Methods Enzymol.* 196:254–264.

27. Akella, J. S., D. Wloga, …, J. Gaertig. 2010. MEC-17 is an alpha-tubulin acetyltransferase. *Nature.* 467:218–222.

28. North, B. J., B. L. Marshall, …, E. Verdin. 2003. The human Sir2 ortholog, SIRT2, is an NAD+-dependent tubulin deacetylase. *Mol. Cell.* 11:437–444.

29. Shida, T., J. G. Cueva, …, M. V. Nachury. 2010. The major alpha-tubulin K40 acetyltransferase alphaTAT1 promotes rapid ciliogenesis and efficient mechanosensation. *Proc. Natl. Acad. Sci. USA.* 107:21517–21522.

30. Gilbert, S. P., M. R. Webb, …, K. A. Johnson. 1995. Pathway of processive ATP hydrolysis by kinesin. *Nature.* 373:671–676.

31. Bulinski, J. C., J. E. Richards, and G. Piperno. 1988. Posttranslational modifications of alpha tubulin: detyrosination and acetylation differentiate populations of interphase microtubules in cultured cells. *J. Cell Biol.* 106:1213–1220.

32. Gundersen, G. G., M. H. Kalnoski, and J. C. Bulinski. 1984. Distinct populations of microtubules: tyrosinated and nontyrosinated alpha tubulin are distributed differently in vivo. *Cell.* 38:779–789.

33. Cambray-Deakin, M. A., and R. D. Burgoyne. 1987. Posttranslational modifications of alpha-tubulin: acetylated and detyrosinated forms in axons of rat cerebellum. *J. Cell Biol.* 104:1569–1574.

34. Cambray-Deakin, M. A., and R. D. Burgoyne. 1987. Acetylated and detyrosinated alpha-tubulins are co-localized in stable microtubules in rat meningeal fibroblasts. *Cell Motil. Cytoskeleton.* 8:284–291.

35. Poole, C. A., Z. J. Zhang, and J. M. Ross. 2001. The differential distribution of acetylated and detyrosinated alpha-tubulin in the microtubular cytoskeleton and primary cilia of hyaline cartilage chondrocytes. *J. Anat.* 199:393–405.

36. Chu, C. W., F. Hou, …, H. Zou. 2011. A novel acetylation of $\beta$-tubulin by San modulates microtubule polymerization via down-regulating tubulin incorporation. *Mol. Biol. Cell.* 22:448–456.

37. Cueva, J. G., J. Hsin, …, M. B. Goodman. 2012. Posttranslational acetylation of $\alpha$-tubulin constrains protofilament number in native microtubules. *Curr. Biol.* 22:1066–1074.

38. Topalidou, I., C. Keller, …, M. Chalfie. 2012. Genetically separable functions of the MEC-17 tubulin acetyltransferase affect microtubule organization. *Curr. Biol.* 22:1057–1065.

39. Howes, S. C., G. M. Alushin, …, E. Nogales. 2014. Effects of tubulin acetylation and tubulin acetyltransferase binding on microtubule structure. *Mol. Biol. Cell.* 25:257–266.

40. Liao, G., and G. G. Gundersen. 1998. Kinesin is a candidate for cross-bridging microtubules and intermediate filaments. Selective binding of kinesin to detyrosinated tubulin and vimentin. *J. Biol. Chem.* 273:9797–9803.

41. Sirajuddin, M., L. M. Rice, and R. D. Vale. 2014. Regulation of microtubule motors by tubulin isotypes and post-translational modifications. *Nat. Cell Biol.* 16:335–344.

42. Erck, C., L. Peris, …, J. Wehland. 2005. A vital role of tubulin-tyrosine-ligase for neuronal organization. *Proc. Natl. Acad. Sci. USA.* 102:7853–7858.